

Rare earth ion doped ceria as electrolytes for solid oxide fuel cell

K.C. Anjaneya¹, J. Manjanna^{1*}, V.M. Ashwin Kumar², H.S. Jayanna³, C.S. Naveen³

¹Department of Industrial Chemistry, Kuvempu University, Shankaraghatta, Karnataka, 577451, India

²Department of Chemistry, Rani Channamma University, Belagavi, Karnataka, 591156, India

³Department of Physics, Kuvempu University, Shankaraghatta, Karnataka, 577451, India

*Corresponding author. Tel: (+91) 8282-256 228; Fax: (+91) 831-2565203; E-mail: jmanjanna@rediffmail.com

Received: 20 July 2015, Revised: 05 February 2016 and Accepted: 25 May 2016

ABSTRACT

We report the nature of rare earth ion doped ceria (REC), $Ce_{0.8}Ln_{0.2}O_{2-\delta}$, ($Ln = Y^{3+}, Gd^{3+}, Sm^{3+}, Nd^{3+}$ and La^{3+}) as oxide ion conductors for their plausible application as electrolytes in intermediate temperature solid oxide fuel cell (SOFC). The samples were prepared by citrate-complexation method and characterized by XRD, SEM/ EDX and UV-Visible spectra. The cubic fluorite-type crystal structure is confirmed from XRD patterns, and the observed lattice parameters are in agreement with calculated values. The UV-Vis spectra of the particles dispersed in aqueous medium showed absorption in the UV region which is ascribed to charge-transfer transition. The dc conductivities at 673 K are in the order of $Ce_{0.8}Sm_{0.2}O_{2-\delta} > Ce_{0.8}Gd_{0.2}O_{2-\delta} > Ce_{0.8}Y_{0.2}O_{2-\delta} > Ce_{0.8}Nd_{0.2}O_{2-\delta} > Ce_{0.8}La_{0.2}O_{2-\delta}$ and their corresponding activation energies are 0.85, 0.87, 0.87, 0.88 and 0.95 eV. Based on ionic and electronic transference numbers, electrical conductivity obtained here is purely ionic, *i.e.*, oxide ion conductors. Copyright © 2016 VBRI Press.

Keywords: Solid oxide fuel cells; oxygen vacancy; chemical synthesis; electrical conductivity.

Introduction

Towards the development of green energy devices, it is essential to improve the performance of solid oxide fuel cells (SOFCs) [1, 2]. Investigations on oxide ion conducting electrolytes are essential to advance the usage of SOFC. Ytria stabilized zirconia (8 mol % Y, YSZ) is widely used as an electrolyte for SOFCs, but it requires high temperature (HT, 1073 K – 1273 K) operation. Also, HT causes severe problems like thermal degradation, thermal expansion mismatch etc [3, 4]. Therefore, development of intermediate temperature (IT, 873 K – 1073 K) SOFC is the current world tendency for SOFC commercialization. Such a reduction in operating temperature of the SOFC is a challenging task. On decreasing the operating temperature, internal resistance of the cell increases tremendously which decreases the performance of cell [5, 6]. Therefore, how to decrease the internal resistance of SOFC is the challenging for IT-SOFCs researchers. Numerous factors lead to the SOFC internal resistance: first and foremost is the large resistance of the current electrolyte materials at IT. Next, the polarization resistances of electrodes (especially cathode) are magnified with the decrease of temperature. There are two possible ways to address these issues: the dimensional thickness of the electrolyte can be reduced to decrease the area specific resistance of the fuel cell and/or developing an electrolyte materials having improved ionic conductivity [7–9]. Therefore, there remains a strong motivation to search for new improved oxygen conducting electrolytes, which can operate at IT. Varieties of oxides are under

investigation like stabilized δ - Bi_2O_3 [10], scandium doped zirconia [11], strontium/magnesium doped lanthanum gallate (LSGM) [12] and doped ceria [13, 14] etc as electrolytes for IT-SOFCs. Among the above IT electrolytes, δ - Bi_2O_3 shows the highest oxygen ion conductivity, but it has little chemical stability as it is reduced at low oxygen partial pressure. Hence, its application in IT-SOFCs is hindered by their limited electrolytic domain [15]. Scandium doped zirconia requires very high sintering temperature and exhibits high internal resistance when operated below 1073 K [16]. Problems of LSGM electrolyte materials at IT includes possible reduction and volatilization of gallium oxide, difficulty in the synthesis of single phase perovskite structure, relatively high cost of gallium, significant reactivity with perovskite electrodes (under oxidizing conditions) as well as with metal anodes in reducing conditions [17, 18]. On other hand, doped ceria is considered as one of the most promising electrolyte material for IT-SOFCs, due to its high oxide ion conductivity and low polarization resistance as well as low cost when compared to YSZ and lanthanum gallate [19, 20].

Experimental

$Ce_{0.8}Ln_{0.2}O_{2-\delta}$ ($Ln = Y^{3+}, Gd^{3+}, Sm^{3+}, Nd^{3+}$ and La^{3+}) solid solutions were synthesized by citrate-complexation method [24]. All the chemicals used in this experiment were analytical grade. Individual solutions of cerium nitrate hexahydrate ($Ce(NO_3)_3 \cdot 6H_2O$, Sigma Aldrich Chemicals), rare earth nitrate hexahydrate ($Ln(NO_3)_3 \cdot 6H_2O$, Sigma

Aldrich Chemicals) were made by dissolving the nitrates in distilled water. Citric acid (Sigma Aldrich Chemicals) was used as chelating agent. 0.08 M of $\text{Ce}(\text{NO}_3)_3 \cdot 6\text{H}_2\text{O}$ and 0.02 M of $\text{Ln}(\text{NO}_3)_3 \cdot 6\text{H}_2\text{O}$ were pre-dissolved in deionized water and then mixed into an aqueous solution at room temperature. The necessary amount of citric acid dissolved in deionized water was then added to the mixed metal nitrate solution with stirring. Mole ratio of total metal ions to citric acid was 1: 2. On heating this mixture on hot plate at 353 K for 4 h, the excess water and nitrate gases were removed to form a transparent and viscous gel. The gel was then transferred to crucible and heated to 573 K for 4 h in a muffle, which led to decomposition of precursors. The residual powder was then calcined at 873 K for 4 h to get final product, designated hereon as YDC20, GDC20, SDC20, NDC20 and LDC20 respectively and stored in desiccators for further use. The samples calcined at 873 K were uniaxially pressed (5 MPa) into pellets of 10 mm in diameter, 2 mm in thickness and sintered at 1473 K in air for 4 h with programmed heating rate of 278 K per minute and cooling rate of 276 K per minute. These high temperature sintered samples were used for density, FE-SEM and dc conductivity measurements.

X-ray diffraction (XRD) pattern of the $\text{Ce}_{0.8}\text{Ln}_{0.2}\text{O}_{2-\delta}$ samples were obtained using a Philips PW 3710 diffractometer (Cu $K\alpha$ radiation) with a step scan of 0.2° . The crystallite size, D , was calculated from the Scherrer's equation: $D = (0.9 \lambda) / (\beta \cos\theta)$, where λ is the wavelength of the X-rays (1.5418 \AA), θ is the angle of main reflection (111) and β is full width at half-maximum intensity (in radians). The lattice parameter $a = d\sqrt{h^2 + k^2 + l^2}$, where $d = \lambda/2\sin\theta$ is the inter planar spacing and θ is the diffraction angle. The lattice parameter a of the RE doped ceria is given by Hong and Virkar [25] as $a = (4x/\sqrt{3}) [r_{\text{Ln}} + (1-x)r_{\text{Ce}} + (1-0.25x)r_{\text{O}} + 0.25x r_{\text{Vo}}] \times 0.9971$, where, x is the concentration of dopant and r_{Ln} , r_{Ce} , r_{O} and r_{Vo} are the radius of dopant cations ($\text{Y}^{3+} = 1.03 \text{ \AA}$, $\text{Gd}^{3+} = 1.05 \text{ \AA}$, $\text{Sm}^{3+} = 1.08 \text{ \AA}$, $\text{Nd}^{3+} = 1.11 \text{ \AA}$ and $\text{La}^{3+} = 1.15 \text{ \AA}$), cerium ion ($\text{Ce}^{4+} = 0.97 \text{ \AA}$), the oxygen ion ($\text{O}^{2-} = 1.38 \text{ \AA}$) and the oxygen vacancy ($r_{\text{Vo}} = 1.164 \text{ \AA}$) respectively. The density of the sintered pellets was determined by standard Archimedes principle. Optical absorption of pure cerium oxide and rare earth doped ceria powders calcined at 873 K were recorded using UV-Vis spectra (UV-1650PC/SHIMADZU). The morphology of the sintered pellets was observed by field-emission scanning electron microscope (FE-SEM-Carl Zeiss, Supra 40 VP) with energy-dispersive X-ray spectroscopy (EDX). The dc electrical conductivity measurements were done using two-probe method (KEITHLEY source meter, Model-2400) in the temperature range of 473 K – 673 K. To prepare samples for the ionic conductivity measurements, silver paste was painted on both sides of sample, followed by baking at 673 K for 1 h. Conductivity was obtained by substituting the value of the resistances and dimensions of the samples in the equation, $\sigma = L/SR$, where, L is the sample thickness, S is the electrode area (sample surface). The ionic (t_{ion}) and electronic (t_{ele}) transference numbers (ionic migration parameters) of the $\text{Ce}_{0.8}\text{Ln}_{0.2}\text{O}_{2-\delta}$ were determined here using KEITHLEY source meter (Model-2400) by Wagner's polarization technique [26] at 673 K in air. For this, the pelletized samples were coated with silver paste on

both sides to construct $\text{Ag}|\text{Ce}_{0.8}\text{Ln}_{0.2}\text{O}_{2-\delta}|\text{Ag}$ cell. The pellet was polarized by supplying a dc voltage of 300 mV for about 4 h.

Results and discussion

The XRD patterns (Fig. 1) of $\text{Ce}_{0.8}\text{Ln}_{0.2}\text{O}_{2-\delta}$ solid solutions matches with the standard cubic fluorite structure with space group Fm3m (JCPDS File No.: 34-0394). A small shift in the ceria peaks depends on the RE-dopant ion indicates the formation of single-phasic solid solutions with a marginal increase in lattice parameter, a ($= 5.411 \text{ \AA}$ for pure CeO_2 [27]).

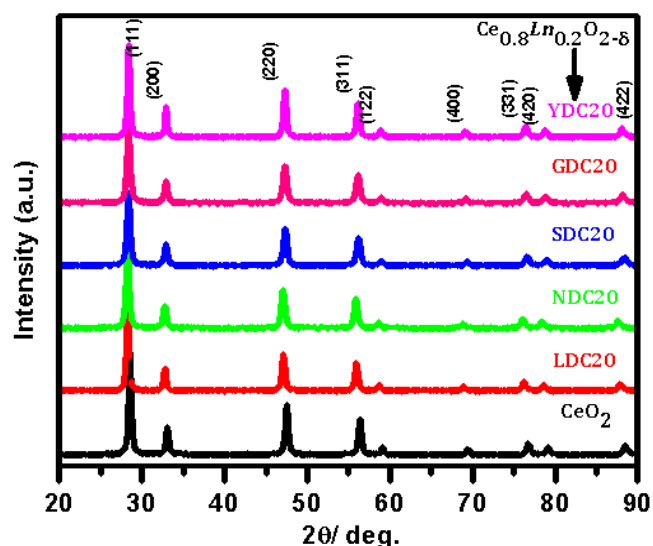


Fig. 1. XRD patterns of REC powders calcined at 873 K for 4 h.

The measured and calculated lattice parameters of $\text{Ce}_{0.8}\text{Ln}_{0.2}\text{O}_{2-\delta}$ as a function of dopant radius are shown in Fig. 2. From the figure, it is clear that the measured lattice parameters are in accordance with calculated lattice parameters. Thus, there is a lattice expansion of CeO_2 structure with increasing radii of the dopant ion.

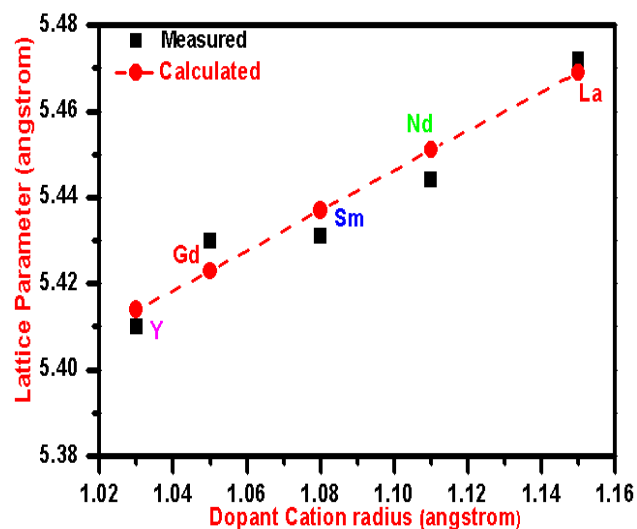


Fig. 2. Measured and calculated lattice parameters of $\text{Ce}_{0.8}\text{Ln}_{0.2}\text{O}_{2-\delta}$ as a function of dopant cation radius.

The crystallite size increases with increasing radius of the dopant from Y^{3+} to Sm^{3+} and then decrease with further increase in size of the dopant ion. Therefore, in $Ce_{0.8}Ln_{0.2}O_{2-\delta}$ crystallite growth strongly depends on the dopant ion. The lattice parameters and crystallite sizes of $Ce_{0.8}Ln_{0.2}O_{2-\delta}$ as a function of dopant radius are given in **Table 1**.

Table 1. Measured, calculated lattice parameters and crystallite sizes of REC as a function of dopant radius.

Composition	Lattice parameter (Å)		Crystallite Size nm
	Measured	Calculated	
$Ce_{0.8}Y_{0.2}O_{2-\delta}$	5.4103	5.4140	21
$Ce_{0.8}Gd_{0.2}O_{2-\delta}$	5.4199	5.4234	22
$Ce_{0.8}Sm_{0.2}O_{2-\delta}$	5.4325	5.4370	24
$Ce_{0.8}Nd_{0.2}O_{2-\delta}$	5.4533	5.4510	19
$Ce_{0.8}La_{0.2}O_{2-\delta}$	5.4721	5.4695	16

UV-Vis spectra of pure CeO_2 and $Ce_{0.8}Ln_{0.2}O_{2-\delta}$ ($Ln = Y^{3+}, Gd^{3+}, Sm^{3+}, Nd^{3+}$ and La^{3+}) samples are shown in **Fig. 3**. Here, all the samples exhibit a strong absorption band below 360 nm, which is due to the charge-transfer transition from O^{2-} (2p) to Ce^{4+} (4f) orbital [28, 29]. The concentration of oxygen vacancies present in solid solution is in relative proportion to the intensity of absorption peak in UV-Vis spectrum. So, the increase of absorption in $Ce_{0.8}Ln_{0.2}O_{2-\delta}$ indicates the substitution of Ce^{4+} with RE cations, such a substitution increases the oxygen vacancy concentration of pure CeO_2 due to charge compensation mechanism [30, 31]. This observation confirms the formation of RE doped ceria solid solutions in corroboration with XRD data.

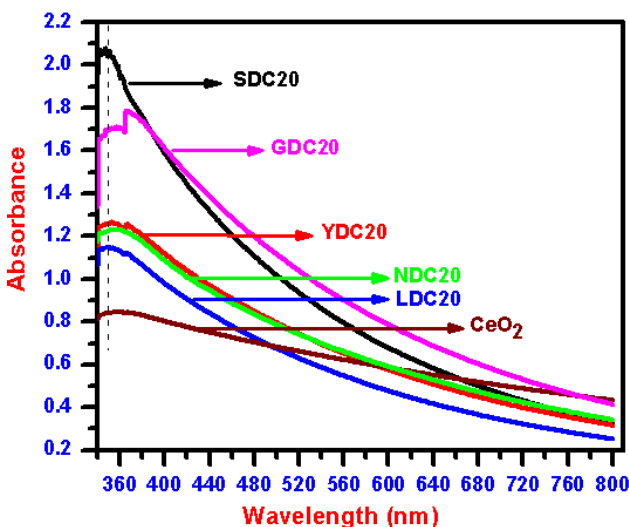


Fig. 3. UV-Visible spectra of $Ce_{0.8}Ln_{0.2}O_{2-\delta}$ solid solutions calcined at 873 K.

Fig. 4 (a-e) shows the EDX spectra for sintered $Ce_{0.8}Ln_{0.2}O_{2-\delta}$ samples, which confirms the desired stoichiometry of all the constituent elements.

Based on the dc conductivity measured by two-probe method, the plots of $\ln(\sigma)$ vs. $1000/T$ for $Ce_{0.8}Ln_{0.2}O_{2-\delta}$ are shown in **Fig. 5**. The ionic conductivity here is the bulk value, which is the sum of grain interior and GB

contributions. The addition of trivalent RE cations into CeO_2 enhances the oxide ionic conductivity by the formation of oxygen vacancies. Among the $Ce_{0.8}Ln_{0.2}O_{2-\delta}$ solid solutions, SDC20 exhibits the maximum electrical conductivity. The ionic conductivities of $Ce_{0.8}Ln_{0.2}O_{2-\delta}$ at 673 K are as follows: $Ce_{0.8}Sm_{0.2}O_{2-\delta} > Ce_{0.8}Gd_{0.2}O_{2-\delta} > Ce_{0.8}Y_{0.2}O_{2-\delta} > Ce_{0.8}Nd_{0.2}O_{2-\delta} > Ce_{0.8}La_{0.2}O_{2-\delta}$. Here the maximum conductivity for SDC20 can be explained in terms of ionic radius ratio (rd/rh) as explained by Kilner [32].

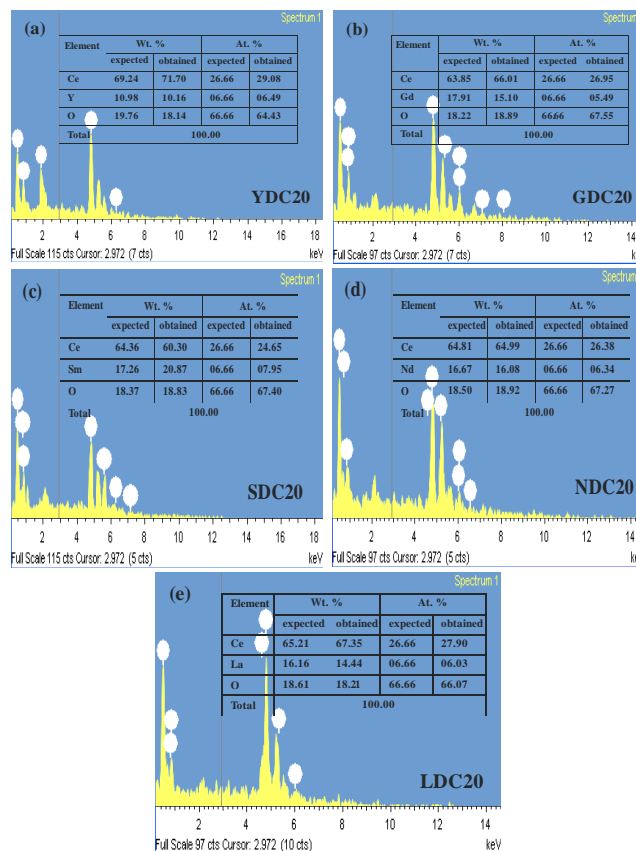


Fig. 4. (a-e) EDX spectra of $Ce_{0.8}Ln_{0.2}O_{2-\delta}$ ($Y^{3+}, Gd^{3+}, Sm^{3+}, Nd^{3+}$ and La^{3+}) pellets sintered at 1473 K.

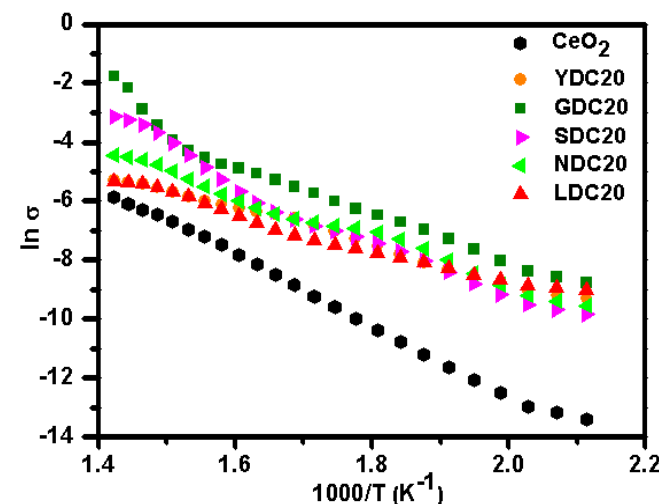


Fig. 5. Arrhenius plots for $Ce_{0.8}Ln_{0.2}O_{2-\delta}$ ($Y^{3+}, Gd^{3+}, Sm^{3+}, Nd^{3+}$ and La^{3+}) solid solutions sintered at 1473 K.

Accordingly, the conductivity is high for those dopants, which are having minimum association enthalpy between the dopant cation and the anion vacancy i.e., r_d/r_h value close to unity. When r_d/r_h approaches to unity, the lattice strain is expected to be minimum, which leads to the increased anion mobility and hence higher conductivity. The r_d/r_h , σ and E_a of $Ce_{0.8}Ln_{0.2}O_{2-\delta}$ at 673 K are given in **Table 2**. As shown in **Table 2**, r_d/r_h close to unity for SDC20 and therefore it exhibits highest conductivity among the $Ce_{0.8}Ln_{0.2}O_{2-\delta}$. However, the global lattice strain is not always a major factor for the high oxide ion conductivity, local structure may be important. Hence, the conductivity also depends on sample preparation method, micro structural feature of sintered pellets, amount of SiO_2 contamination and RE cations segregating at GB. In the present citrate method, the amount of SiO_2 contamination and RE cations segregating at GB is low in comparison to other methods such as solid-state reaction [33, 34] etc. Both the amount of SiO_2 contamination and the RE cations segregating to GBs may have a significant effect on the dc conductivity. Here for SDC20, SiO_2 contamination and Sm cations segregating at GBs might be lowest and also SDC20 contain more continuous GB phases than those of GDC20, NDC20, LDC20 and YDC20. Hence, SDC20 exhibits highest conductivity among the RE doped ceria solid solutions, which is in corroboration with Kilner theory.

Table 2. Dopant radius, radius ratio (r_d/r_h), conductivity (σ_t) and activation energy (E_a) of $Ce_{0.8}Ln_{0.2}O_{2-\delta}$ (Y^{3+} , Gd^{3+} , Sm^{3+} , Nd^{3+} and La^{3+}) solid solutions.

Sample	Radius ratio r_d/r_h	At 673 K	
		Conductivity σ_t ($S\text{cm}^{-1}$)	Activation energy E_a (eV)
$Ce_{0.8}Y_{0.2}O_{2-\delta}$	1.11	1.69×10^{-4}	0.87
$Ce_{0.8}Gd_{0.2}O_{2-\delta}$	1.08	1.88×10^{-4}	0.87
$Ce_{0.8}Sm_{0.2}O_{2-\delta}$	1.06	2.36×10^{-3}	0.85
$Ce_{0.8}Nd_{0.2}O_{2-\delta}$	1.14	1.36×10^{-4}	0.88
$Ce_{0.8}La_{0.2}O_{2-\delta}$	1.18	5.54×10^{-5}	0.95

The activation energy (E_a) is calculated from the slope of the straight line plot of $\ln(\sigma)$ vs. $1000/T$. The E_a for dc conductivity was found to be 0.85, 0.87, 0.87, 0.88 and 0.95 eV for Sm, Gd, Y, Nd and La doped ceria respectively, which indicates that all the solid solutions are oxide ion conductors. **Fig 6** shows the variation of E_a and conductivity as function of RE dopant radius. As can be seen, the E_a decreases with increase in radius from Y^{3+} to Sm^{3+} , then increases consistent with the results of total conductivity as shown in **Fig 5**. The changes in E_a on dopant radius seems to be correlated with conductivity variations with dopant radius i.e. the maximum value of total conductivity corresponds to the minimum E_a in agreement with the Meyer-Neldel compensation rule [35].

The ion migration parameters such as ionic (t_{ion}) and electronic (t_{ele}) transference numbers of $Ce_{0.8}Ln_{0.2}O_{2-\delta}$ are determined here by Wagner's polarization technique at 673 K in air. Based on the current values measured by programmable multimeter, t_{ion} and t_{ele} transference numbers are calculated by using the equations: $t_{ion} = (I_i - I_f) / I_i$ and t_{ele}

$= I_f / I_i$, where I_i is the initial current and I_f is the final current. For all $Ce_{0.8}Ln_{0.2}O_{2-\delta}$ samples, the t_{ion} and t_{ele} transference numbers are > 0.90 and < 0.10 respectively. This suggests that the electrical transport in these solid electrolytes is mainly due to ions and the material is ionic in nature.

Based on the above preliminary investigations, for IT-SOFCs electrolytes the selection of dopant is very important parameter, which in turn influence on the conductivity of samples. Nevertheless, other electrochemical and mechanical properties such as open circuit voltage and thermal expansion constants must be considered for the selection of proper dopant as electrolyte materials for IT-SOFCs.

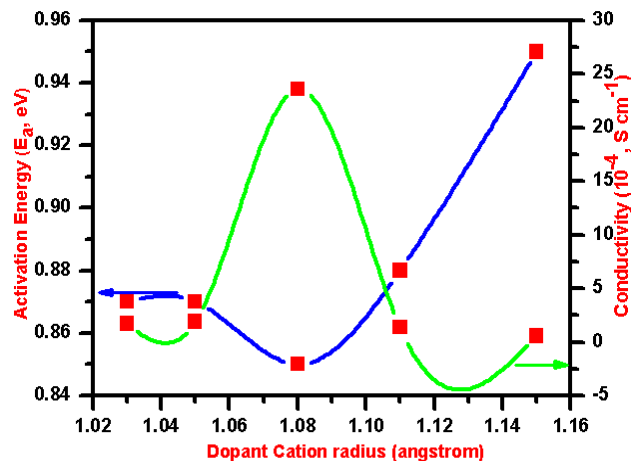


Fig. 6. Variation of activation energy (E_a) and conductivity (σ) as a function of dopant cation radius for $Ce_{0.8}Ln_{0.2}O_{2-\delta}$ ($Ln = Y^{3+}$, Gd^{3+} , Sm^{3+} , Nd^{3+} and La^{3+}) solid solutions.

Conclusion

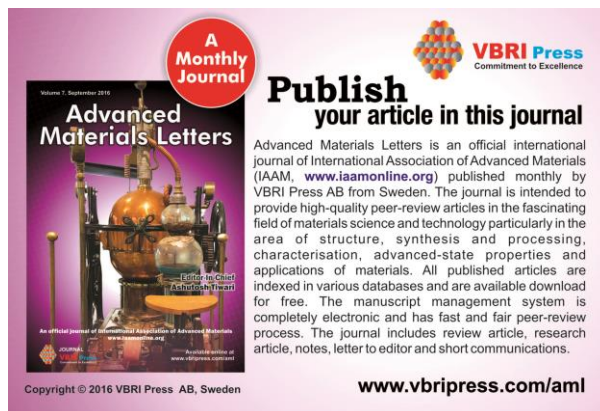
The lattice parameters, ionic conductivity, activation energy and ionic migration parameters of rare earth ion doped ceria (REC), $Ce_{0.8}Ln_{0.2}O_{2-\delta}$ ($Ln = Y^{3+}$, Gd^{3+} , Sm^{3+} , Nd^{3+} and La^{3+}), prepared by citrate complexation, are determined. XRD data confirm their cubic fluorite-type structure with space group $Fm\bar{3}m$, and the measured lattice parameters were in accordance with calculated values. UV-Vis spectra also confirm the formation of REC solid solutions. EDXA shows the expected stoichiometry of all the constituent elements. Sm doped ceria exhibits highest oxygen ion conductivity ($2.36 \times 10^{-3} S\text{cm}^{-1}$) when compared to Gd, Y, Nd and La doped samples. The ionic conductivities value at 673 K are in the order of $Ce_{0.8}Sm_{0.2}O_{2-\delta} > Ce_{0.8}Gd_{0.2}O_{2-\delta} > Ce_{0.8}Y_{0.2}O_{2-\delta} > Ce_{0.8}Nd_{0.2}O_{2-\delta} > Ce_{0.8}La_{0.2}O_{2-\delta}$ and their corresponding activation energies are 0.85, 0.87, 0.87, 0.88 and 0.95 eV. The change in activation energy with conductivity follows the Meyer-Neldel compensation rule. Ion migration parameter revealed that, these solid electrolytes were ionic nature. It is clear from these studies that the selection of proper dopant is very important to get high conductivity and good electrochemical characteristics. Based on this preliminary investigation, we propose these REC solid solutions as potential electrolytes for IT-SOFCs.

Acknowledgements

One of the authors (K.C. Anjaneya) gratefully acknowledges the financial support from the Kuvempu University (Grant No. KU: Ph.D: IC: 08 (1243) 22-02-2012).

References

- Zhang, X.; Liu, L.; Zhao, Z.; Tu, B.; Ou, D.; Cui, D.; Wei, X.; Cheng, M; *Nano Lett.*, **2015**, *15*, 1703.
DOI: [10.1021/nl5043566](https://doi.org/10.1021/nl5043566)
- Ruic-Morales, J.C.; Marrero-López, D.; Gálvez-Sánchez, M.; Canales-Vázquez, J.; Savaniu, C.; Savvin, S.N; *Energy Environ. Sci.*, **2010**, *3*, 1670.
DOI: [10.1039/C0EE00166J](https://doi.org/10.1039/C0EE00166J)
- Zheng, Y.; Zhou, M.; Ge, L.; Li, S.; Chen, H.; Guo, L; *J. Alloys Compd.*, **2011**, *509*, 1244.
DOI: [10.1016/j.jallcom.2010.09.203](https://doi.org/10.1016/j.jallcom.2010.09.203)
- Minh, N.Q; *J. Am. Ceram. Soc.*, **1993**, *76*, 563.
DOI: [10.1111/j.1151-2916.1993.tb03645.x](https://doi.org/10.1111/j.1151-2916.1993.tb03645.x)
- Acharya, S.A; *J. Power Sources*, **2012**, *198*, 105.
DOI: [10.1016/j.jpowsour.2011.09.087](https://doi.org/10.1016/j.jpowsour.2011.09.087)
- Zhang, Y.; He, S.; Ge, L.; Zhou, M.; Chan, H.; Guo, L; *Int. J. Hydrogen Energy*, **2011**, *36*, 5128.
DOI: [10.1016/j.ijhydene.2011.01.042](https://doi.org/10.1016/j.ijhydene.2011.01.042)
- Breet, D.J.; Atkinson, A.; Brandon, N.P.; Skinner, S.J; *Chem. Soc. Rev.*, **2008**, *37*, 1568.
DOI: [10.1039/B612060C](https://doi.org/10.1039/B612060C)
- Huijser, A.; Schoonman; *J. Environ. Eng. Manage. J.*, **2005**, *4*, 293.
DOI: <http://omicron.ch.tuiasi.ro/EEMJ/2005>
- Beckel, D.; Huetter, A.B.; Harvey, A.; Infortuna, A.; Muecke, U.P.; Prestat, M.; Rupp, J.L.M.; Gaucker, L.J; *J. Power Sources*, **2005**, *173*, 325.
DOI: [10.1016/j.jpowsour.2007.04.070](https://doi.org/10.1016/j.jpowsour.2007.04.070)
- Kharton, V.V.; Naumovich, E.N.; Yaremchenko, A.A.; Marques, F.M.B; *J. Solid State Electrochem.*, **2001**, *5*, 160.
DOI: [10.1007/s100080000141](https://doi.org/10.1007/s100080000141)
- Kulkarni, S.; Duttgupta, S.; Phatak, G; *RSC Adv.*, **2014**, *4*, 46602.
DOI: [10.1039/C4RA06602B](https://doi.org/10.1039/C4RA06602B)
- Feng, M.; Goodenough, J.B; *Eur. J. Solid State Inorg. Chem.*, **1994**, *31*, 663.
DOI: [10.1016/j.ss.inorchem.100060000011](https://doi.org/10.1016/j.ss.inorchem.100060000011)
- Fu, Y.P.; Chen, S.H.; Huang, J.J; *Int. J. Hydrogen Energy*, **2010**, *35*, 745.
DOI: [10.1016/j.ijhydene.2009.10.093](https://doi.org/10.1016/j.ijhydene.2009.10.093)
- Jamshidijam, M.; Mangalaraja, R.V.; Akbari-Fakhrabadi, A.; Ananthakumar, S.; Chen, S.H; *Powder. Tech.*, **2014**, *253*, 304.
DOI: [10.1016/j.powtec.2013.10.032](https://doi.org/10.1016/j.powtec.2013.10.032)
- Takahashi, T.; Iwahara, H; *Mater. Res. Bull.*, **1978**, *13*, 1447.
DOI: [10.1016/0025-5408\(78\)90138-1](https://doi.org/10.1016/0025-5408(78)90138-1)
- Ralph, J. M.; Schoeler, A.C.; Krumpelt, M; *J. Mater. Sci.*, **2001**, *36*, 1161.
DOI: [10.1023/A:1004881825710](https://doi.org/10.1023/A:1004881825710)
- Djurado, E.; Labeau, M; *J. Eur. Ceram. Soc.*, **1998**, *18*, 1397.
DOI: [10.1016/S0955-2219\(98\)00016-8](https://doi.org/10.1016/S0955-2219(98)00016-8)
- Yamaji, K.; Horita, T.; Ishikawa, M.; Sakai, N.; Yokokawa, H; *Solid State Ionics*, **1999**, *121*, 217.
DOI: [10.1016/S0167-2738\(99\)00039-9](https://doi.org/10.1016/S0167-2738(99)00039-9)
- Kuharungrong, S; *J. Power Sources*, **2007**, *171*, 506.
DOI: [10.1016/j.jpowsour.2007.05.104](https://doi.org/10.1016/j.jpowsour.2007.05.104)
- Murray, E.P.; Tsai, T.; Barnett, S.A; *Nature*, **1999**, *400*, 649.
DOI: [10.1038/232220](https://doi.org/10.1038/232220)
- Guang, L.J.; Takayasu, I.; Toshiyuki, M; *Acta. Mater.*, **2004**, *52*, 2221.
DOI: [10.1016/j.actamat.2004.01.014](https://doi.org/10.1016/j.actamat.2004.01.014)
- Balaguier, M.; Soils, C.; Serra, J.M; *J. Phys. Chem. C.*, **2012**, *116*, 7975.
DOI: [10.1021/jp211594d](https://doi.org/10.1021/jp211594d)
- Fuentes, R.O.; Baker, R.T; *Int. J. Hydrogen Energy*, **2008**, *33*, 3480.
DOI: [10.1016/j.ijhydene.2007.10.026](https://doi.org/10.1016/j.ijhydene.2007.10.026)
- Muccillo, E.N.S.; Rocha, R.A.; Muccillo, R. *Mater. Lett.*, **2002**, *53*, 353.
DOI: [10.1016/S0167-577X\(01\)00506-7](https://doi.org/10.1016/S0167-577X(01)00506-7)
- Hong, S.J.; Virkar, A.V; *J. Am. Ceram. Soc.*, **1995**, *78*, 433.
DOI: [10.1111/j.1151-2916.1995.tb08820.x](https://doi.org/10.1111/j.1151-2916.1995.tb08820.x)
- Wagner, J.B.; Wagner, C; *J. Chem. Phys.*, **1957**, *26*, 1597.
DOI: [10.1063/1.1743590](https://doi.org/10.1063/1.1743590)
- Weber, W.H.; Hass, K.C.; McBride, J.R; *Phys. Rev. B.*, **1993**, *48*, 178.
DOI: [10.1103/PhysRevB.48.178](https://doi.org/10.1103/PhysRevB.48.178)
- Guo, M.; Lu, J.; Wu, Y.; Wang, Y.; Luo, M; *Langmuir*, **2011**, *27*, 3872.
DOI: [10.1021/la200292f](https://doi.org/10.1021/la200292f)
- Li, L.; Chen, F.; Lu, J.Q.; Luo, M.F; *J. Phys. Chem. C.*, **2011**, *115*, 7972.
DOI: [10.1021/jp203921m](https://doi.org/10.1021/jp203921m)
- Li, G.; Qu, D.; Arurault, L.; Tong, Y; *J. Phys. Chem C.*, **2009**, *113*, 1235.
DOI: [10.1021/jp804572t](https://doi.org/10.1021/jp804572t)
- Kuntaiah, K.; Sudarsanam, P.; Reddy, B.M.; Vinu, A; *RSC Adv.*, **2013**, *3*, 7953.
DOI: [10.1039/C3RA23491F](https://doi.org/10.1039/C3RA23491F)
- Kilner, J.A; *Solid State Ionics*, **1983**, *8*, 201.
DOI: [10.1016/0167-2738\(83\)90017-6](https://doi.org/10.1016/0167-2738(83)90017-6)
- Pikalova, E.Y.; Murashkina, A.A.; Maragou, V.I.; Demin, A.K.; Strekalovskay, V.N.; Tsiakaras, P.E; *Int. J. Hydrogen Energy*, **2011**, *36*, 6175.
DOI: [10.1016/j.ijhydene.2011.01.132](https://doi.org/10.1016/j.ijhydene.2011.01.132)
- Eguchi, K.; Setoguchi, T.; Inoue, T.; Arai, H; *Solid State Ionics*, **1992**, *52*, 165.
DOI: [10.1016/0167-2738\(92\)90102-U](https://doi.org/10.1016/0167-2738(92)90102-U)
- Fang, P.H; *Phys. Lett. A.*, **1969**, *30*, 217.
DOI: [10.1016/0375-9601\(69\)90863-9](https://doi.org/10.1016/0375-9601(69)90863-9)



A Monthly Journal

Publish your article in this journal

Advanced Materials Letters is an official international journal of International Association of Advanced Materials (IAAM, www.iaamonline.org) published monthly by VBRI Press AB from Sweden. The journal is intended to provide high-quality peer-review articles in the fascinating field of materials science and technology particularly in the area of structure, synthesis and processing, characterisation, advanced-state properties and applications of materials. All published articles are indexed in various databases and are available download for free. The manuscript management system is completely electronic and has fast and fair peer-review process. The journal includes review article, research article, notes, letter to editor and short communications.

www.vbripress.com/aml

Copyright © 2016 VBRI Press AB, Sweden